Article

A Synthetic Analog of the Mineral Ivanyukite: Sorption Behavior to Lead Cations

Gleb O. Samburov [1,*], Galina O. Kalashnikova [2], Taras L. Panikorovskii [1], Vladimir N. Bocharov [3], Aleksandr Kasikov [4], Ekaterina Selivanova [2,5], Ayya V. Bazai [2,5], Daria Bernadskaya [6], Viktor N. Yakovenchuk [2,4] and Sergey V. Krivovichev [2]

1 Laboratory of Nature-Inspired Technologies and Environmental Safety of the Arctic, Kola Science Centre, Russian Academy of Sciences, 184209 Apatity, Russia; t.panikorovskii@ksc.ru

2 Nanomaterials Research Centre, Kola Science Centre, Russian Academy of Sciences, 184209 Apatity, Russia; g.kalashnikova@ksc.ru (G.O.K.); selivanova@geoksc.apatity.ru (E.S.); bazai@geoksc.apatity.ru (A.V.B.); yakovenchuk@geoksc.apatity.ru (V.N.Y.); s.krivovichev@ksc.ru (S.V.K.)

3 Geo Environmental Centre "Geomodel", Saint-Petersburg State University, 198504 St. Petersburg, Russia; bocharov@molsp.phys.spbu.ru

4 I.V. Tananaev Institute of Chemistry and Technology of Rare Elements and Mineral Raw Materials, Kola Science Centre, Russian Academy of Sciences, 184209 Apatity, Russia; a.kasikov@ksc.ru

5 Geological Institute, Kola Science Centre, Russian Academy of Sciences, 184209 Apatity, Russia

6 Institute of the North Industrial Ecology Problems, Kola Science Centre, 184209 Apatity, Russia; d.bernadskaya@ksc.ru

* Correspondence: g.samburov@ksc.ru; Tel.: +7-921-030-88-75

Abstract: The production of electrolytic nickel includes the stage of leaching of captured firing nickel matte dust. The solutions formed during this process contain considerable amounts of Pb, which is difficult to extraction due to its low concentration upon the high-salt background. The sorption of lead from model solutions with various compositions by synthetic and natural titanosilicate sorbents (synthetic ivanyukite-Na-*T* (SIV), ivanyukite-Na-*T*, and AM-4) have been investigated. The maximal sorption capacity of Pb is up to 400 mg/g and was demonstrated by synthetic ivanyukite In solutions with the high content of Cl$^-$ (20 g/L), extraction was observed only with a high amount of Na (150 g/L). Molecular mechanisms and kinetics of lead incorporation into ivanyukite were studied by the combination of single-crystal and powder X-ray diffraction, microprobe analysis, and Raman spectroscopy. Incorporation of lead into natural ivanyukite-Na-*T* with the *R*3m symmetry by the substitution $2Na^+ + 2O^{2-} \leftrightarrow Pb^{2+} + \square + 2OH^-$ leds to its transformation into the cubic *P*−43*m* Pb-exchanged form with the empirical formulae $Pb_{1.26}[Ti_4O_{2.52}(OH)_{1.48}(SiO_4)_3]\cdot3.32(H_2O)$.

Keywords: ivanyukite; lintisite; SIV; AM-4; synthesis; sorption; lead; ion-exchange; titanosilicate; Arctic

1. Introduction

Minerals of the ivanyukite group were discovered in 2009 by Yakovenchuk and co-authors in a pegmatite vein of the Koashva apatite mine, Khibiny Massif, Kola Peninsula, Russia [1]. Ivanyukite group minerals have been found in several variaties including ivanyukite-Na-*T* (*T*—rigonal form), ivanyukite-Na-*C* (*C*—cubic form), ivanyukite—K, and ivanyukite—Cu. The observed chemical diversity was assigned to the high ion-exchange and sorption capacities of the minerals.

In contrast to othertitanosilicates discovered in the Khibiny Massif or Lovozero Massif (Kola Peninsula, Russia)—such as lintisite, zorite and sitinakite [2–7]—the synthetic of ivanyukite was was known prior to its mineralogical discovery, being obtained by D. Chapman and A. Roe in 1990 [8] under the name name 'grace titanium silicate' (GTS). For their synthesis process, the authors had used $Ti(OC_2H_5)_4$ as a source of Ti. The synthetic titanosilicate AM-4 was first obtained by M.S. Dadachov in 1997 using $TiCl_3$ as a starting reagent [9].

In this work, the synthesis of ivanyukite and AM-4 was done using different Ti sources. For example, semi-product ($TiCl_4$) of hydrochloric acid loparite ore treatment (JSC "Solikamsk Magnesium Works", Solikamsk, Russia) [10] and a semi-product (ammonium titanylsulfate $(NH_4)_2TiO(SO_4)_2 \cdot H_2O$) of sulfuric acid titanite ore treatment (mining JSC "Apatit", PhosAgro, Russia) [11,12] were used extensively, providing a link between industrially available compounds and a new material with potential innovative applications.

There are human health risks associated with the lead exposure and are important for industrial areas and surrounding cities. For example, in the Monchegorsk city area (Kola peninsula) the nickel and copper pollution is by 6–1500 times higher than the European background levels [13]. Analysis of trace metals by atomic adsorption spectroscopy [14] showed that the highly Pb-polluted waters of the Kola Peninsula reached 425-times the background concentration (8 μg/L) in areas of anthropogenic impact compared to the background level of the Murmansk region [14]. The concentration of Pb is more than 19-times higher than the reference recommended values of maximum tolerable concentrations of this element in soils around copper–nickel metallurgical smelters [15–17].

Since this work was carried out taking into account the principle of integrated nature management, one of the subjects of research was both models and real samples of solutions of the nickel–copper plant JSC "Severonickel KMM" (Monchegorsk, Russia). These solutions are characterized by a low concentrations of Ag and Pb cations (0.3 g/L and up to 1 g/L, respectively) with the high concentrations of NaCl or $NaSO_4$ (up to 200 g/L).

For the purification of silver-containing solutions, a new technique has been developed and a patent application RU 2021124566A has been filed [16]. In this work, we propose new conditions (molar ratio, temperature, and volume) for the synthesis of the AM-4 and SIV titanosilicates and test their sorption properties with respect to Pb for different solutions. The molecular mechanism and kinetics of Pb incorporation into ivanyukite structure has been studied here in detail.

2. Materials and Methods

2.1. Materials and Their Abbreviations

SIV—is a synthetic titanosilicate material with the composition $Na_4(TiO)_4(SiO_4)_3 \cdot nH_2O$ that possesses a microporous crystal structure similar to that observed in ivanyukite-group minerals [1].

AM-4—is a synthetic analog of the mineral lintisite that is used in this work for comparison of its sorption properties with those of SIV was obtained according to the methodology described in detail in [3,18,19].

SL3—is the protonated form of AM-4 obtained according to the methods described in [3,18].

STA—is ammonium sulfate oxytitanium, $(NH_4)_2TiO(SO_4)_2 \cdot H_2O$, the pre-product of titanite concentrate reprocessing (PJSC "PhosAgro", Apatity, Russia) [20].

2.2. Reagents

Titanium tetrachloride (JSC "Solikamsk Magnesium Works", Solikamsk, Russia) and $(NH_4)_2TiO(SO_4)_2 \cdot H_2O$ (PJSC PhosAgro, Apatity, Russia) were of technical grade quality; sodium hydroxide (Aldrich, Moscow, Russia) was of ACS grade quality; sodium metasilicate, lead nitrate, and sodium chloride produced by the Neva Reactive were of U.S.P. grade quality. The solutions 1–7 were model and real solutions after processing (leaching) of fine dusts of nickel production generated by the pyrometallurgical processes at metallurgical plants and captured by electrostatic precipitators during dry cleaning of dust and gas phases.

2.3. Synthesis

Sodium metasilicate and titanium tetrachloride (or ammonium sulfate oxytitanium) were taking according to they molar ratios of $Na_2O:SiO_2:TiO_2:H_2O$ = 4.5:4:1:160 [9,16] and 5.6:3.1:1:128, for the synthesis of SIV and of AM-4, respectively. The mixture of initial reagents was dissolved in a distilled water at 298 K and stirred with the mixing speed of

200 revolutions per minute during 4 h to obtain SIV powders. The autoclaves with the mixtures were maintained under hydrothermal conditions (453 K, 1.5 MPa) for 96 h (in the case of $TiCl_4$) and 48 h (in the case of ammonium sulfate oxytitanium). The product were filtered by vacuum flask, washed by distilled water (1/5 of the total mixture volume), and dried at 348 K.

Autoclaves with the volumes of 40 cm^3 and 450 cm^3 (production of FRC Kola Science Centre, Apatity, Russia) were used for the hydrothermal synthesis of the SIV. The autoclave with volume of 7 L (Parr Instrument Company, Moline, IL, USA) was used for SIV synthesis only. TheSIV powders were firstly obtained with the initial molar ratio of $Na_2O:SiO_2:TiO_2:H_2O = 5.6:3.1:1:128$ under 373 K.

The high precision universal drying oven SNOL (SNOL-TERM, Utena, Lithuania), with the operating temperature range from 323 to 573 K and programmable thermostat, was used for heating autoclaves and for power drying.

The synthesized powders were separated from the mother liquor by vacuum filtration using a diaphragm pump (Technology for Vacuum system, Vacuubrand, Wertheim, Germany).

In all cases where mixing was necessary, a magnetic stirrer IKA RT 5 (Germany) was used.

The drying process of the powder was carried out for 4 h at 348 K using the SNOL drying oven (SNOL-TERM, Utena, Lithuania).

Sartorius—ED224S-RCE (Sartorius, Goettingen, Germany) was the first class accuracy analytical balance used for weighing synthetic titanosilicate powders and reagents.

2.4. Composition

Investigation of morphology of the Pb-exchanged ivanyukite samples was carried out using a scanning electron microscope LEO-1450 (Carl Zeiss Microscopy, Oberkochen, Germany) and chemical composition was studied with an Oxford Instruments Ultim Max 100 analyzer at 20 kV, 500–1000 pA, 1–3 μm beam diameter (Geological Institute of Kola Science Centre, Apatity, Russia).

The content of Pb in the samples was determined by the inductively coupled plasma atomic emission spectrometry (ICP AES, Institute of the North Industrial Ecology Problems of Kola Science Centre, Apatity, Russia). To construct the calibration curve, a multi-element standard sample of Pb^{2+} ions GSO 7877-2000 was used. The samples were diluted with 2% nitric acid in a ratio of 1:100. The 2% nitric acid was obtained by mixing purified water—18.2 MΩ × cm (Ultra Clear TP UV UF TM, EVOQUA, Pittsburgh, PA, USA) with distilled nitric acid obtained by an acid distillation unit (SPK-2, Saint-Petersburg, Russia).

The obtained solutions were analyzed by an "Optima 2100 DV" (PerkinElmer, Waltham, MA, USA) an inductively coupled plasma atomic emission spectrometer with the following settings: wavelength 220.353 nm; axial torch viewing position; nebulizer gas flow 0.8 L/min; flow rate 1.5 mL/min; power 1300 Watts (Institute of the North Industrial Ecology Problems of Kola Science Centre, Apatity, Russia). The method of standard addition was used to estimate the validity of the analysis.

2.5. Pb Sorption from the Simulated Model Solution

The possibility of extracting Pb from its solutions by employing titanosilicates was studied using nitrate salt. For this purpose, the $Pb(NO_3)_2$ solutions containing 0.39, 0.88, and 1.79 g/L of Pb (initial solutions 1–3) were prepared by dissolving in 1000 cm^3 of distilled water 0.62, 1.4, and 2.87 g of $Pb(NO_3)_2$ respectively. The sorption experiments were conducted by the immersion of titanosilicate powders into solutions at 298 K for 4 h with a constant stirring. The ratio of liquid and solid phases was V:m = 50:0.5 (mL:g) in each experiment. After sorption, the powders were filtered by vacuum filtration, washed with distilled water in three steps (50 mL for each step), and dried at 348 K. For each experiment, a parallel control experiment was conducted.

2.6. Pb Sorption from the Dust Leaching Solution (Model Solution)

Before starting work with a real solution of leaching of nickel Feinstein firing dusts, an experiment was conducted on a model solution, simulating the composition of industrial solutions. In order to prepare the latter, 60 mL of NaCl solution with the concentration 333 g/L (20 g NaCl dissolved in 60 mL of distilled water) and 20 mL of $Pb(NO_3)_2$ solution with a concentration 6.5 g/L (0.13 g $Pb(NO_3)_2$ dissolved in 20 mL of distilled water) were added with a small portion of 20 mL $AgNO_3$ solution at a concentration of 0.8 g/L (0.016 g $AgNO_3$ dissolved in 20 mL of distilled water); the resulting solution was diluted in 400 mL of Na_2SO_4 solution with a concentration of 95 g/L. The experimental conditions agreed well with the conditions described for the experiments with a model solution $Pb(NO_3)_2$ with a difference in a liquid–solid ratio, which in this case was equal to V:m = 25:0.25 (cm^3:g). The SL3 sorbent was not used in the experiments with the first model solutions because of its low efficiency in recent studies. For each experiment, a parallel control experiment was conducted.

2.7. Pb Sorption from the Dust Leaching Solution (Real Solution)

Two different solutions of leaching of fine dusts of nickel production firing dusts from copper-nickel plant JSC "Severonickel KMM" were used in this study as provided by the industrial plant laboratory. The first one, solution-6, was obtained by the treatment the fine-grained dust of nickel production with a solution of sodium chloride with the concentration of 200 g/L and precipitation of Pb with a solution of sodium sulphate with the concentration 200 g/L. The second one, solution-7, was a product of the dusts of nickel production treatment similar to solution-6, except for that leaching was carried out with a solution of sulfuric acid with the concentration of 200 g/L. The conditions of the sorption experiments were same as those implemented for model solutions.

For each experiment, a second parallel experiment was conducted for control purposes.

The cation-exchange capacity of the sorbent (mg/g) in each experiment was calculated by Equation (1)

$$q = (C_0 - C_e) \cdot (V/m) \tag{1}$$

where C_0—is the initial concentration of the element in the solution (mg/L); C_e—is the equilibrium concentration of the element in the solution after sorption (mg/L); V—is the volume of solution (L); m—is the mass of the sorbent (g).

The extent of extraction of the element (%) was calculated by Equation (2)

$$A = \frac{C_0 - C_e}{C_0} \cdot 100 \tag{2}$$

where C_0—the initial concentration of the element in the solution (mg/L); C_e—the equilibrium concentration of the element in the solution after sorption (mg/L).

2.8. Raman Spectroscopy

The Raman spectra (RS) of SIV, SIV-Pb, and Pb-exchanged form of ivanyukite collected from uncoated individual grains were recorded with a Horiba Jobin-Yvon LabRAM HR800 spectrometer (Horiba, Kyoto, Japan) equipped with an Olympus BX-41 microscope (Olympus Corporation, Tokyo, Japan) in backscattering geometry (Saint-Petersburg State University, Saint-Petersburg, Russia). Raman spectra were excited by a solid-state laser (532 nm) with an actual power of 2 mW under the $50\times$ objective (NA 0.75). The spectra were obtained in a range of 70–4000 cm^{-1} at a resolution of 2 cm^{-1} at room temperature. To improve the signal-to-noise ratio, the number of acquisitions was set to 15. The spectra were processed using the algorithms implemented in Labspec (Horiba, Kyoto, Japan) and OriginPro 8.1 (OriginLab Corporation, Northampton, MA, USA) software packages.

2.9. Powder and Single-Crystal X-ray Diffraction

The synthetic products were investigated by means of powder X-ray diffraction using a Bruker D2 Phaser diffractometer (Bruker Corporation, Billerica, MA, USA) (Cu$K\alpha$ radiation, 30 kV/10 mA) (XRD Research Center, St. Petersburg State University, Saint-Petersburg, Russia). The experiments were carried out in the 2θ range 5–65 (°) with a step of 0.02°, and the exposure at each point was 1 s.

The crystal-structure study of Pb-exchanged ivanyukite was carried out at the X-ray Diffraction Resource Centre of St. Petersburg State University (Saint-Petersburg, Russia) by means of the Synergy S single-crystal diffractometer equipped with a Hypix (Rigaku Corporation, Tokyo, Japan) detector using monochromatic Mo$K\alpha$ radiation (λ = 0.71069 Å) at room temperature. More than a half of the diffraction sphere was collected with scanning step of 1°, and an exposure time of 30 s. The data were integrated and corrected by means of the CrysAlis (Rigaku Corporation, Tokyo, Japan) program package, which was also used to apply empirical absorption correction using spherical harmonics, implemented in the SCALE3 ABSPACK scaling algorithm [21]. The structure was refined using the SHELXL software package [21]. The crystal structure was drawn using the VESTA 3 program [22]. Occupancies of the cation sites were calculated from the experimental site-scattering factors (except for the low-occupied sites) in accordance with the empirical chemical composition. Hydrogen sites could not be located.

The SCXRD data are deposited in CCDC under entry no. 2130913. Crystal data, data collection information, and refinement details are given in Table 1. Atom coordinates and isotropic parameters of atomic displacements are given in Table S1, interatomic distances in Table S2, and the anisotropic parameters of atomic displacements are given in Table S3.

Table 1. Crystal data, data collection information, and refinement details Pb-exchanged form ivanyukite.

Temperature/K	293 (2)
Crystal system	cubic
Space group	*P*-43m
$a = b = c/$Å	7.8037 (7)
$\alpha = \beta = \gamma/°$	90
Volume/Å^3	475.23 (13)
Z	1
ρ_{calc}g/cm^3	2.956
μ/mm^{-1}	13.003
F (000)	388.0
Crystal size/mm^3	0.12 × 0.12 × 0.12
Radiation	Mo Kα (λ = 0.71073)
2θ range for data collection/°	7.384 to 52.998
Index ranges	$-6 \leq$ h ≤ 9, $-9 \leq$ k ≤ 4, $-9 \leq$ l ≤ 9
Reflections collected	612
Independent reflections	200 [R_{int} = 0.0486, R_{sigma} = 0.0310]
Data/restraints/parameters	200/0/23
Goodness-of-fit on F^2	1.116
Final R indexes [I $\geq 2\sigma$ (I)]	R_1 = 0.0497, wR_2 = 0.1186
Final R indexes [all data]	R_1 = 0.0644, wR_2 = 0.1257
Largest diff. peak/hole/e Å^{-3}	0.71/−0.64
Flack parameter	0.008(19)

3. Results

3.1. Composition

Natural ivanyukite contains numerous intergrowths of aegirine (Figure 1a). Pb-exchanged natural ivanyukite contains up to 0.04 apfu of Fe^{2+} and 0.12 apfu of Nb^{5+}, whereas its synthetic counterpart may contain up to 0.09 apfu of Al^{3+}. The SIV aggregates are represented by a fine-grained matrix with nanometer-sized crystallites (Figure 1b). AM-

4 forms rosette-like aggregates with the size of individual crystals less than $100 \times 100 \times 10$ μm (Figure 1f). Both samples of Pb-exchanged SIV and AM-4 (Figure 1c,e) contained an admixtures of prismatic crystals of Pb_3O_4 (Figure 1d).
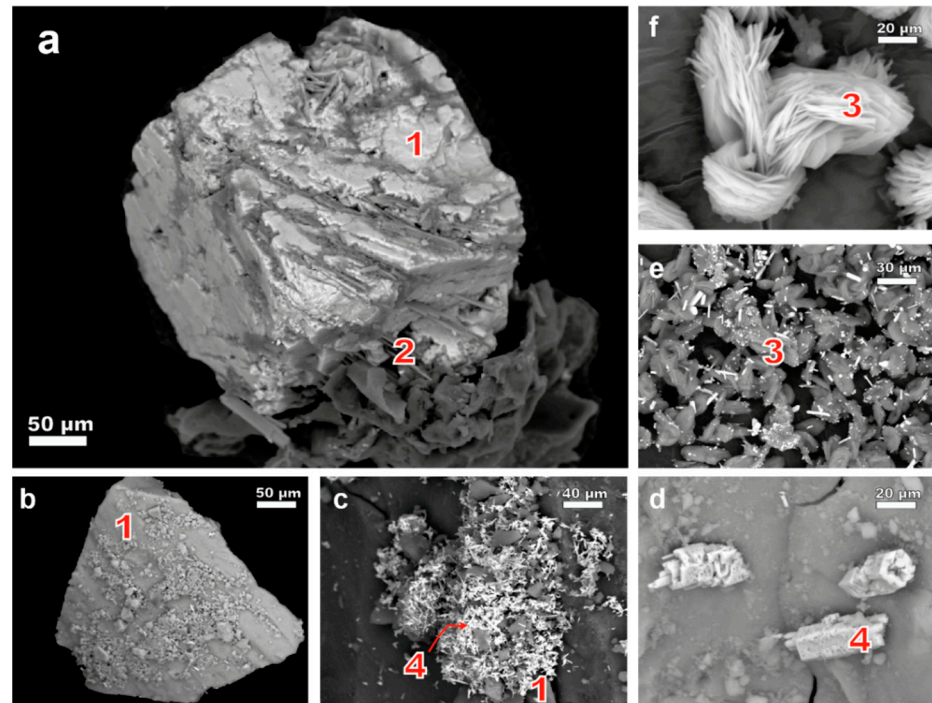

Figure 1. Backscattered images of (**a**) Pb-exchanged natural ivanyukite (1) with aegirine (2) inclusion; (**b**) Pb-exchanged SIV; (**c**) formation of Pb_3O_4 (4) crystals on the surface Pb-exchanged SIV; (**d**) individual prismatic crystals of Pb_3O_4; (**e**) Pb-exchanged AM-4 (3); (**f**) AM-4rosette-like aggregates.

The Pb-exchanged SIV contains residual 0.06–0.36 apfu of K^+. Both synthetic and natural ivanyukite demonstrate exceptional ion-exchange properties close to the ideal substitution scheme $2Na^+ \leftrightarrow 1Pb^{2+} + 1\square$. Table 2 provides analytical results for natural and synthetic ivanyukite and their Pb-exchanged forms.

Table 2. Chemical composition of Pb-exchanged SIV and Pb-exchanged natural ivanyukite.

Constituent	Pb-Exchanged SIV			Pb-Exchanged Natural Ivanyukite	
SiO_2	18.11	19.08	19.40	18.23	19.23
TiO_2	30.74	30.01	31.64	31.65	32.50
Al_2O_3	0.45		0.23		
FeO				0.22	0.31
Nb_2O_5				1.64	1.68
K_2O	0.44	0.32	1.85		
PbO	38.60	38.40	36.03	37.59	34.87
H_2O *	9.70	10.00	11.00	10.10	10.10
Total	98.04	97.81	100.15	99.43	98.69
Si^{4+}	3.00	3.00	3.00	3.00	3.00
Ti^{4+}	3.83	3.55	3.68	3.92	3.81
Al^{3+}	0.09		0.04		
Fe^{2+}				0.03	0.04
Nb^{5+}				0.12	0.12
Sum O	3.92	3.55	3.72	4.07	3.97

Table 2. *Cont.*

Constituent	Pb-Exchanged SIV			Pb-Exchanged Natural Ivanyukite	
K$^+$	0.09	0.06	0.36		
Pb^{2+}	1.72	1.63	1.50	1.67	1.46
Sum A	1.81	1.69	1.86	1.67	1.46
OH$^-$	10.72	10.49	11.35	11.09	10.51

* The content of H_2O was calculated according to the ivanyukite formula (4 apfu) and the content of OH according to the charge-balance requirements.

3.2. Pb Sorption from the Simulated Model Solution

The concentrations of Pb in the model solutions were determined by atomic emission spectrometry and are given in Table 3.

Table 3. Results of sorption experiments of Pb from $Pb(NO_3)_2$ solutions.

	C(Pb), g/L	q, mg/g	A, %
Initial solution 1	0.39		
SIV	0.0089	38.11	97.72
SL3	0.31	8	20.51
AM-4	0.0008	38.92	99.79
Initial solution 2	0.88		
SIV	0.004	87.6	99.55
SL3	0.80	8	9.09
AM-4	0.0009	87.91	99.90
Initial solution 3	1.79		
SIV	0.0026	178.74	99.85
AM-4	0.0009	178.91	99.95
Initial solution 4	1.78		
SIV	0.97	403	45.28
AM-4	1.73	26	2.92
Initial solution 5 *	0.16		
SIV	0.016	14.4	90
AM-4	0.017	14.3	89
Initial solution 6 *	23.70		
SIV	0.11	2.4	99.5
AM-4	<0.03	2.4	99.9
Initial solution 7 *	56.23		
SIV	55.04	0.1	2.1
AM-4	55.68	0.1	1.0

* Data on the sorption of silver from solutions are not given due to the registration of the patent RU 2021124566 [17].

The cation-exchange capacity of the sorbents with respect to Pb was up to 178 mg/g for SIV and AM-4 with the extent of extraction of up to 99.85% and 8 mg/g for SL3 in each solution (initial solutions 1–3). In all cases the extent of extraction of Pb by the SIV and AM-4 was more than 99%.

It was found that, under given conditions for Pb sorption from the industrial solutions, both sorbents demonstrated excellent sorption properties with respect to Pb (Table 3, initial solution 5). The cation-exchange capacity for Pb was 14.4 and 14.3 mg/g for SIV and AM-4, respectively, with the extents of extraction equal to 90%.

The extent of Pb extraction from the real dust leaching solution-6 was 99.55% with the cation-exchange capacity for SIV equal to of 13 mg/g. The results of the experiment are presented in Table 3.

3.3. Raman Spectroscopy

The Raman spectra of SIV (ivanyukite-Na-*T*), SIV-Pb, and Pb-exchanged natural ivanyukite are shown in Figure 2. The assignments of the absorption bands were made by analogy with structurally related pharmacosiderite type compounds [23–25] and titanosilicates [26–29].
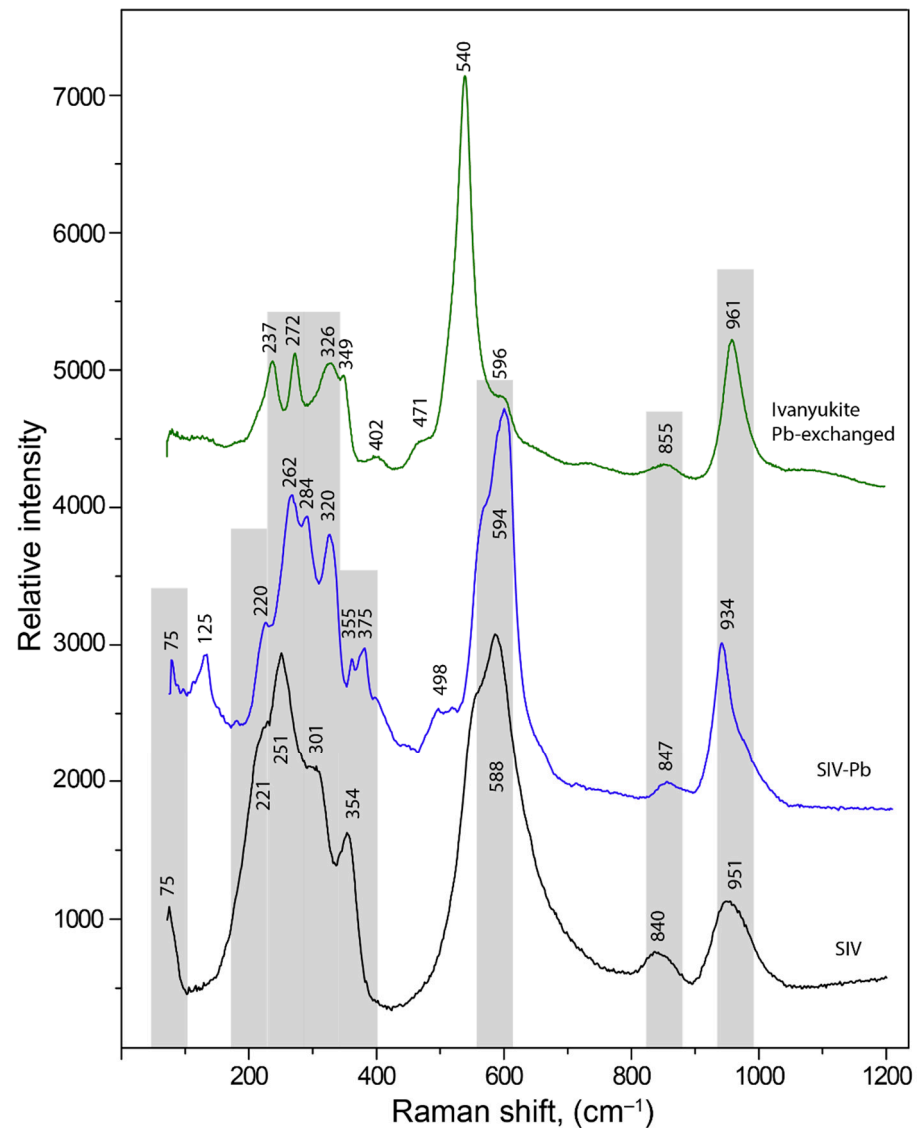

Figure 2. Raman spectra of initial SIV, SIV-Pb, and Pb-exchanged natural ivanyukite. The main bands in the initial SIV spectra are indicated by gray lines.

The intense vibrational bands at 951, 934, and 961 cm^{-1} can be attributed to asymmetric stretching vibrations of SiO_4 tetrahedra, while the bands at 840, 847, and 855, cm^{-1} are assigned to symmetric vibration modes involving the same bonds [24,28]. The most intense bands at 588 and 594 cm^{-1} for rhombohedral SIV are significantly shifted (by ~60 cm^{-1}) in comparison with the band at 540 cm^{-1} observed in the spectrum of Pb-exchanged natural ivanyukite and are related to the asymmetric bending vibrations of Si–O bonds or overlapping stretching vibrations of Ti–O bonds [25,28]. The same shift was observed previously for natural ivanyukite and corresponded to the transition from rhombohedral to cubic form [27]. The bands in the range of 350–500 cm^{-1} correspond to symmetric bending vibrations of O–Si–O bonds and overlapping stretching vibrations of Ti–O bonds [25–27]. The bands at 498 and 471 cm^{-1} were assigned to different modes of Ti–O stretching

vibrations. Bands of different intensities in the region of 200–350 cm^{-1} belong to different bending vibration modes of the Ti–O bonds in TiO$_6$ octahedra [23,24]. The bands with the wave numbers below 200 cm^{-1} belong to translational vibrations. The bands at 75 and 126–128 cm^{-1} are observed in the Raman spectra of synthetic samples and are absent in the Raman spectrum of the Pb-exchanged natural ivanyukite and probably respond to translation modes of K.

In general, the spectrum of Pb-exchanged natural ivanyukite corresponds to the cubic form, whereas the spectrum of SIV-Pb has characteristic features corresponding to both trigonal and cubic forms. It contains bands near 498 cm^{-1} that are characteristic of cubic Pb-exchanged natural ivanyukite and at the same time has bands near 220 and 350 cm^{-1} that are characteristic of trigonal SIV. This can be explained by the presence of domains with both trigonal and cubic symmetries within the single grains of SIV-Pb.

3.4. Powder Diffraction

The initial XRD pattern of SIV is in good agreement with that of synthetic ivanyukite-Na-*T*, (PDF Card No. 00-052-1204). Intensity of the (101) reflection significantly decreases after Pb sorption (Figure 3). The appearance of (440) reflection at 68.18°2θ (1.3743 Å) in SIV-Pb instead two peaks at 67.15 and 68.80°2θ observed in SIV pattern indicates the *R*3m to *P*−43*m* symmetry change. The observed pattern for the Pb-exchanged SIV agrees with that of synthetic ivanyukite-Na-*C* (PDF Card No.00-047-0042). The increase in the Pb concentration results in the decrease of intensities of main reflections and is probably connected with the increase of absorption coefficient induced by the increases amounts of Pb in the structure. When the maximum sorption capacity is reached, the Pb$_3$O$_4$ lead oxide (PDF Card No. 01-071-0562) starts to crystallize. The presence of Pb$_3$O$_4$ was confirmed by our chemical data (Figure 1d) and the presence of additional reflections at 24.82°2θ (3.584 Å), 25.49°2θ (3.492 Å), and 43.48°2θ (2.079 Å).
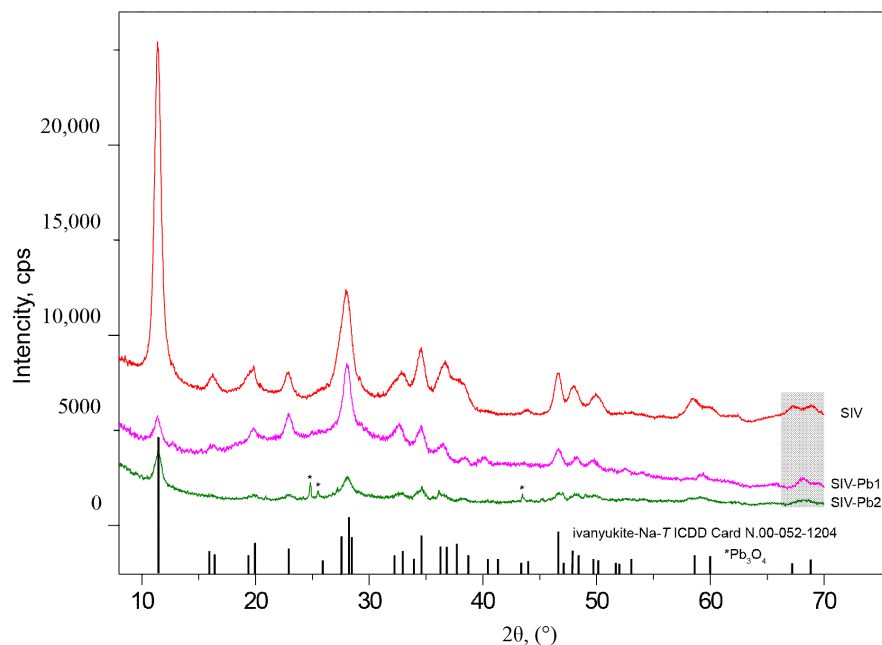

Figure 3. Diffraction patterns of SIV (red curve) and its Pb-exchanged forms with the S:L ratios of 1:500 (pink) and 1:133 (green). Asterisks indicate peaks of Pb$_3$O$_4$.

3.5. Single-Crystal XRD

The crystal structure of Pb-exchanged ivanyukite was refined in the *P*−43*m* space group to R_1 = 0.049 for 200 (R_{int} = 0.049, R_{sigma} = 0.030) independent reflections with $F_o > 4\sigma(F_o)$ using the model of ivanyukite-K [27]. The crystal structure of Pb-exchanged ivanyukite (Figure 4a) possesses a pharmacosiderite structural topology and is based upon

a topologically identical three-dimensional framework [28]. The main structural feature of ivanyukite-group minerals is the presence of cubane-like $[Ti_4O_4]^{8+}$ clusters formed by four edge-sharing TiO_6 octahedra [29]. The $[Ti_4O_4]^{8+}$ clusters are connected by sharing corners with SiO_4 tetrahedra to form a negatively charged $[(TiO)_4(SiO_4)_3]_{4-}$ framework. The framework has a three-dimensional system of channels defined by 8-membered rings (8-MRs) with a free (suitable for migration) crystallographic diameter of ~3.5 Å [30]. The channels are occupied by extra-framework cations (e.g., Na^+, K^+) and H_2O molecules.
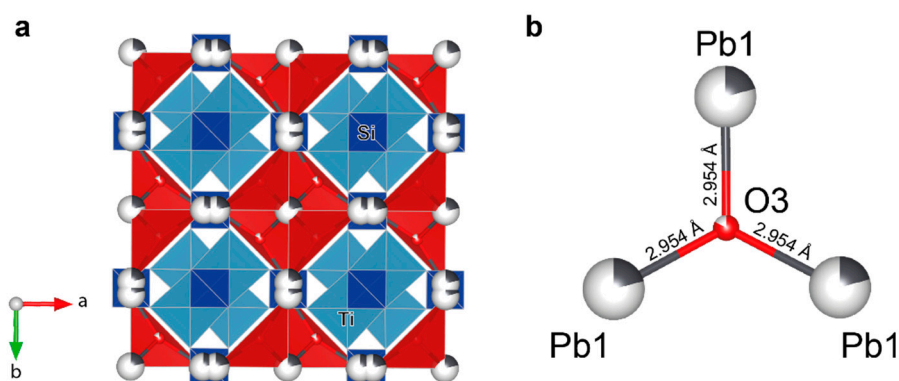
Figure 4. Crystal structure of Pb-exchanged ivanyukite in general projection (**a**); local coordination of Pb in the crystal structure of Pb-exchanged ivanyukite (**b**).

In the crystal structure of Pb-exchanged ivanyukite, as in other cubicpharmacosiderite-supergroup minerals [31], there is one symmetrically independent Si1 and one Ti1 site coordinated by the O1 and O2 atoms. The mean bond lengths for SiO_4 tetrahedra TiO_6 octahedra are, <1.642> Å and <1.961> Å, respectively, in good agreement with their full occupancies. The splitted Pb1 site is situated at the center of the 8-MR with the site occupation factor (s.o.f.) = of 0.21 and the Pb−Pb distance of 0.62 Å. The Pb1 site is bonded to two $O3(H_2O)$ sites.

The structural formula of Pb-exchanged ivanyukite determined from the structure refinement can be written as $Pb_{1.26}[Ti_4O_{2.52}(OH)_{1.48}(SiO_4)_3]\cdot 3.32(H_2O)$.

4. Discussion

Incorporation of Pb into natural ivanyukite-Na-*T* by the substitution scheme $2Na^+ + 2O^{2-} \leftrightarrow Pb^{2+} + \square + 2OH^-$ results in its transformation into the cubic Pb-exchanged form. The same transition with increasing symmetry from $R3m$ to $P-43m$ was observed for the synthetic material and confirmed by powder X-ray diffraction (Figure 3) and Raman spectroscopy (Figure 2). During the Pb sorption, the significant decrease of the (101) reflection intensity and the appearance of additional peak at 68.18°2θ, instead of two peaks at 67.15 and 68.80°2θ, was observed. In the Raman spectra the shift for the most intense band at 580–600 cm^{-1} to 500–540 cm^{-1} related to the asymmetric bending vibrations of Si–O bonds or overlapping stretching vibrations of Ti–O bonds was observed. Such a shift was previously described for similar transitions in the ivanyukite-group minerals [27].

According to our chemical and sorption data, the maximal sorption capacity in relation to Pb was demonstrated by synthetic ivanyukite and reaches 400 mg/g at ambient conditions with synthetic ivanyukite. The maximal Pb content reaches 1.71 apfu. In the crystals structure of Pb-exchanged ivanyukite, the Pb1 site is situated at the center of the 8-MR and participates in the OPb_3 triangles with the O−Pb distance of 2.954 Å (Figure 4b). Oxocentred triangles OA_3 (A = metal) are typical structural units in bismuth oxysalts with additional oxygen atoms [31,32], and was observed in Pb oxysalts as well [33].

There is a certain balance between the amounts of Pb in precipitates and the remaining solution. At the same time, there is an observed dependence of these amount from the NaCl content that is usually introduced at the beginning of the dust leaching process. When Na^+ concentration is up to 200 g/L, the precipitation of Pb is seemingly incomplete. When the

Na$^+$ concentration is more than 200 g/L, no additional precipitation of trace amounts of Pb was observed.

In the case of the studied solutions, strongly acidic medium (pH < 1) the fast protonation reactions in SIV and AM-4 titanosilicates is favored. In this case, Na$^+$ cations should be quickly leaching into solution and two concurrent processes are observed described by the equations $2Na^+ + O^{2-} \leftrightarrow 2\square + OH$ (protonation) and $2Na^+ \leftrightarrow Pb^{2+}$ (ion-exchange).

It is known that Pb^{2+} cations in acidic chloride-sulfate solutions of metallurgical industries can form stable anionic complexes—such as $[PbCl_3]^-$, $[PbCl_4]^{2-}$, $[PbCl_6]^{4-}$, among others—which can be extracted from a solution on anion exchangers (e.g., AMP or AM-2b) with –CH$_2$N$^+$, –CH$_2$N(CH$_3$)$_2$, and –CH$_2$N(CH$_3$)$_3$ serving the role of exchange groups [34,35]. The sorption of Pb from acid mine drainage also includes its association to organic hydroxyl and carboxyl, SiO$_4$$^{2-}$, and –R–O–H functional groups [36,37]. The presence of carboxyl groups in some clay minerals also improves the adsorption of Pb [38]. In the case of titanosilicates used in this work, the key-role is presumably played by extra-framework sodium cations, which displacement may significantly affect the change in the surface charge of the samples. The SL3 material in this case is a good example of the formation of an intermediate between the product and the initial AM-4 phase leading to the change in the nature of the active centers of the material (decrease in the acidic strength of the active centers as a result of protonation) [19]. Since SL3 did not prove to be a good sorbent for Pb in our studies, we can assume that titanosilicate samples containing Na$^+$ are required to decrease the stability of lead chloride complexes. In solutions with the content of Cl$^-$ (20 g/L), extraction is observed with a high background of sodium in the solution (150 g/L) only. For this reason, it is important to determine and fix the mechanisms of the reactions taking place in natural ivanyukite crystals.

5. Conclusions

Occurrence of extra framework Na$^+$ cations in the structure of titanosilicate sorbents plays a key role in Pb sorption. Both AM-4, Na$_2$Ti$_2$[Si$_4$O$_{13}$(OH)]·2H$_2$O and SIV, Na$_3$Ti$_4$(SiO$_4$)$_3$O$_4$·4H$_2$O titanosilicates with extra framework Na$^+$ cations demonstrate 90% to 99% of Pb extraction from different solutions. At the same time SL3, Ti$_2$[Si$_4$O$_{10}$(OH)$_4$]—protonated modification of AM-4 does not demonstrate good sorption properties. The maximal sorption capacity with respect to Pb is demonstrated by SIVand reaches 400 mg/g at ambient conditions. Both AM-4 and SIV may be recommended for the Pb sorption from the Pb-bearing dust leaching solution.

In solutions with the content of Cl$^-$ (20 g/L), extraction was observed only with the high background of Na (150 g/L). It seems that Na$^+$ ions neutralize Cl$^-$, which catalyzes the exchange reaction.

The molecular mechanism of incorporation of Pb^{2+} into ivanyukite structure by the substitution scheme $2Na^+ + 2O^{2-} \leftrightarrow Pb^{2+} + \square + 2OH^-$ result in the structure transition with increasing symmetry from $R3m$ to $P-43m$. The symmetry transition has been confirmed by the SC XRD, PXRD, and Raman data. In the crystal structure of Pb-substituted form, Pb^{2+} cations occupy the centers of the 8-MRs and forms oxo-centered OPb$_3$ units.

6. Patents

Nikolaev, A.I.; Samburov, G.O.; Kalashnikova, G.O.; Kasikov, A.G.; Panikorovskii, T.L.; Bazai, A.V. Method of silver extraction from pyrometallurgical wastes. Patent application RU 2021124566A, 16 February 2022.

Supplementary Materials: The following are available online at https://www.mdpi.com/article/10.3390/cryst12030311/s1, Table S1: Fractional Atomic Coordinates ($\times 10^4$) and Equivalent Isotropic Displacement Parameters (Å^2 × 10^3) for Pb-exchanged ivanyukite. U$_{eq}$ is defined as 1/3 of the trace of the orthogonalised U$_{IJ}$ tensor; Table S2: Anisotropic Displacement Parameters (Å^2 × 10^3) for Pb-exchanged ivanyukite. The Anisotropic displacement factor exponent takes the form: $-2\pi^2[h^2a \times {}^2U_{11} + 2hka \times b \times U_{12} + \ldots]$; Table S3: Bond Lengths for Pb-exchanged ivanyukite.

References

1. Yakovenchuk, V.N.; Nikolaev, A.P.; Selivanova, E.A.; Pakhomovsky, Y.A.; Korchak, J.A.; Spiridonova, D.V.; Zalkind, O.A.; Krivovichev, S.V. Ivanyukite-Na-T, ivanyukite-Na-C, ivanyukite-K, and ivanyukite-Cu: New microporous titanosilicates from the Khibiny massif (Kola Peninsula, Russia) and crystal structure of ivanyukite-Na-T. *Am. Mineral.* **2009**, *94*, 1450–1458. [CrossRef]
2. Popa, K.; Pavel, C.C.; Bilba, N.; Cecal, A. Purification of waste waters containing $60Co^{2+}$, $115mCd^{2+}$ and $203Hg^{2+}$ radioactive ions by ETS-4 titanosilicate. *J. Radioanal. Nucl. Chem.* **2006**, *269*, 155–160. [CrossRef]
3. Kalashnikova, G.O.; Zhitova, E.S.; Selivanova, E.A.; Pakhomovsky, Y.A.; Yakovenchuk, V.N.; Ivanyuk, G.Y.; Kasikov, A.G.; Drogobuzhskaya, S.V.; Elizarova, I.R.; Kiselev, Y.G.; et al. The new method for obtaining titanosilicate AM-4 and its decationated form: Crystal chemistry, properties and advanced areas of application. *Microporous Mesoporous Mater.* **2021**, *313*, 110787. [CrossRef]
4. Cruciani, G.; De Luca, P.; Nastro, A.; Pattison, P. Rietveld refinement of the zorite structure of ETS-4 molecular sieves. *Microporous Mesoporous Mater.* **1998**, *21*, 143–153. [CrossRef]
5. Anthony, R.G.; Dosch, R.G.; Gu, D.; Philip, C.V. Use of silicotitanates for removing cesium and strontium from defense waste. *Ind. Eng. Chem. Res.* **1994**, *33*, 2702–2705. [CrossRef]
6. Men'shikov, Y.P.; Sokolova, E.V.; Egorov-Tismenko, Y.K.; Khomyakov, A.P.; Polezhaeva, L.I. Sitinakite, $Na_2KTi_4Si_2O_{13}(OH) \cdot 4H_2O$— A new mineral. *Zap. RMO* **1992**, *121*, 94–99. (In Russian)
7. Panikorovskii, T.L.; Kalashnikova, G.O.; Nikolaev, A.I.; Perovskiy, I.A.; Bazai, A.V.; Yakovenchuk, V.N.; Bocharov, V.N.; Kabanova, N.A.; Krivovichev, S.V. Ion-Exchange-Induced Transformation and Mechanism of Cooperative Crystal Chemical Adaptation in Sitinakite: Theoretical and Experimental Study. *Minerals* **2022**, *12*, 248. [CrossRef]
8. Chapman, D.M.; Roe, A.L. Synthesis, characterization and crystal chemistry of microporous titanium-silicate materials. *Zeolites* **1990**, *10*, 730–737. [CrossRef]
9. Dadachov, M.; Rocha, J.; Ferreira, A.; Lin, Z.; Anderson, M. Ab initio structure determination of layered sodium titanium silicate containing edge-sharing titanate chains (AM-4) $Na_3(Na,H)Ti_2O_2[Si_2O_6]_2 \cdot 2H_2O$. *Chem. Commun.* **1997**, *3*, 2371–2372. [CrossRef]
10. Britvin, S.N.; Gerasimova, L.G.; Ivanyuk, G.Y.; Kalashnikova, G.O.; Krzhizhanovskaya, M.G.; Krivovivhev, S.V.; Mararitsa, V.F.; Nikolaev, A.I.; Oginova, O.A.; Panteleev, V.N.; et al. Application of titanium-containing sorbents for treating liquid radioactive waste with the subsequent conservation of radionuclides in Synroc-type titanate ceramics. *Theor. Found. Chem. Eng.* **2016**, *50*, 598–606. [CrossRef]

11. Gerasimova, L.; Nikolaev, A.; Maslova, M.; Shchukina, E.; Samburov, G.; Yakovenchuk, V.; Ivanyuk, G. Titanite Ores of the Khibiny Apatite-Nepheline-Deposits: Selective Mining, Processing and Application for Titanosilicate Synthesis. *Minerals* **2018**, *8*, 446. [CrossRef]
12. Gerasimova, L.G.; Nikolaev, A.I.; Shchukina, E.S.; Maslova, M.V. Hydrothermal synthesis of framed titanosilicates with a structure of ivanyukite mineral. *Доклады Академии наук* **2019**, *487*, 289–292. [CrossRef]
13. Barcan, V.; Sylina, A. The appraisal of snow sampling for environmental pollution valuation. *Water. Air. Soil Pollut.* **1996**, *89*, 49–65. [CrossRef]
14. Yakovlev, E.; Druzhinina, A.; Druzhinin, S.; Zykov, S.; Ivanchenko, N. Assessment of physical and chemical properties, health risk of trace metals and quality indices of surface waters of the rivers and lakes of the Kola Peninsula (Murmansk Region, North-West Russia). *Environ. Geochem. Health* **2021**, 1–30. [CrossRef]
15. Barcan, V.; Kovnatsky, E. Soil Surface Geochemical Anomaly Around the Copper-Nickel Metallurgical Smelter. *Water. Air. Soil Pollut.* **1998**, *103*, 197–218. [CrossRef]
16. Koptsik, G.N.; Koptsik, S.V.; Smirnova, I.E.; Sinichkina, M.A. Remediation of Technogenic Barren Soils in the Kola Subarctic: Current State and Long-Term Dynamics. *Eurasian Soil Sci.* **2021**, *54*, 619–630. [CrossRef]
17. Nikolaev, A.I.; Samburov, G.O.; Kalashnikova, G.O. Method for the Extraction of Silver from Pyrometallurgical Waste. RU Patent Application No. 2021124566A, 16 February 2022.
18. Merlino, S.; Pasero, M.; Khomyakov, A.P. The crystal structure of lintisite, $Na_3LiTi_2[Si_2O_6]_2O_2 \cdot 2H_2O$, a new titanosilicate from Lovozero (USSR). *Z. Krist.* **1990**, *193*, 137–148. [CrossRef]
19. Timofeeva, M.N.; Kalashnikova, G.O.; Shefer, K.I.; Mel'gunova, E.A.; Panchenko, V.N.; Nikolaev, A.I.; Gil, A. Effect of the acid activation on a layered titanosilicate AM-4: The fine-tuning of structural and physicochemical properties. *Appl. Clay Sci.* **2020**, *186*, 105445. [CrossRef]
20. Gerasimova, L.G.; Shchukina, E.S.; Maslova, M.V.; Gladkikh, S.N.; Garaeva, G.R.; Kolobkova, V.M. Synthesis of rutile titanium dioxide from Russian raw materials. *Polym. Sci. Ser. D* **2017**, *10*, 23–27. [CrossRef]
21. Sheldrick, G.M. Crystal structure refinement with SHELXL. *Acta Crystallogr. Sect. C Struct. Chem.* **2015**, *71*, 3–8. [CrossRef]
22. Momma, K.; Izumi, F. VESTA 3 for three-dimensional visualization of crystal, volumetric and morphology data. *J. Appl. Crystallogr.* **2011**, *44*, 1272–1276. [CrossRef]
23. Frost, R.L.; Kloprogge, J.T. Raman spectroscopy of some complex arsenate minerals—implications for soil remediation. *Spectrochim. Acta Part A Mol. Biomol. Spectrosc.* **2003**, *59*, 2797–2804. [CrossRef]
24. Filippi, M. Oxidation of the arsenic-rich concentrate at the Přebuz abandoned mine (Erzgebirge Mts., CZ): Mineralogical evolution. *Sci. Total Environ.* **2004**, *322*, 271–282. [CrossRef]
25. Filippi, M.; Doušová, B.; Machovič, V. Mineralogical speciation of arsenic in soils above the Mokrsko-west gold deposit, Czech Republic. *Geoderma* **2007**, *139*, 154–170. [CrossRef]
26. Yakovenchuk, V.; Pakhomovsky, Y.; Panikorovskii, T.; Zolotarev, A.; Mikhailova, J.; Bocharov, V.; Krivovichev, S.; Ivanyuk, G. Chirvinskyite, $(Na,Ca)_{13}(Fe,Mn,\square)_2(Ti,Nb)_2(Zr,Ti)_3$-$(Si_2O_7)_4(OH,O,F)_{12}$, a New Mineral with a Modular Wallpaper Structure, from the Khibiny Alkaline Massif (Kola Peninsula, Russia). *Minerals* **2019**, *9*, 219. [CrossRef]
27. Pakhomovsky, Y.A.; Panikorovskii, T.L.; Yakovenchuk, V.N.; Ivanyuk, G.Y.; Mikhailova, J.A.; Krivovichev, S.V.; Bocharov, V.N.; Kalashnikov, A.O. Selivanovaite, $NaTi_3(Ti,Na,Fe,Mn)_4[(Si_2O_7)_2O_4(OH,H_2O)_4] \cdot nH_2O$, a new rock-forming mineral from the eudialyte-rich malignite of the Lovozero alkaline massif (Kola Peninsula, Russia). *Eur. J. Mineral.* **2018**, *30*, 525–535. [CrossRef]
28. Krivovichev, S. Topology of Microporous Structures. *Rev. Mineral. Geochem.* **2005**, *57*, 17–68. [CrossRef]
29. Panikorovskii, T.L.; Yakovenchuk, V.N.; Yanicheva, N.Y.; Pakhomovsky, Y.A.; Shilovskikh, V.V.; Bocharov, V.N.; Krivovichev, S.V. Crystal chemistry of ivanyukite-group minerals, $A_{3-x} H_{1+x} [Ti_4O_4 (SiO_4)_3](H_2O)_n$ (A = Na, K, Cu), (n = 6–9, x = 0–2): Crystal structures, ion-exchange, chemical evolution. *Mineral. Mag.* **2021**, *85*, 607–619. [CrossRef]
30. Oleksiienko, O.; Wolkersdorfer, C.; Sillanpää, M. Titanosilicates in cation adsorption and cation exchange—A review. *Chem. Eng. J.* **2017**, *317*, 570–585. [CrossRef]
31. Rumsey, M.S.; Mills, S.J.; Spratt, J. Natropharmacoalumite, $NaAl_4[(OH)_4(AsO_4)_3] \cdot 4H_2O$, a new mineral of the pharmacosiderite supergroup and the renaming of aluminopharmacosiderite to pharmacoalumite. *Mineral. Mag.* **2010**, *74*, 929–936. [CrossRef]
32. Bedlivy, D.; Mereiter, K. Preisingerite, $Bi_3O(OH)(AsO_4)_2$, a new species from San Juan Province, Argentina: Its description and crystal structure. *Am. Mineral.* **1982**, *67*, 833–840.
33. Ridkosil, T.; Srein, V.; Fabry, J.; Hybler, J.; Maximov, B.A. Mrazekite, $Bi_2Cu_3(OH)_2O_2(PO_4)_2$. *Can. Mineral.* **1992**, *30*, 215–224.
34. Siidra, O.I.; Zinyakhina, D.O.; Zadoya, A.I.; Krivovichev, S.V.; Turner, R.W. Synthesis and Modular Structural Architectures of Mineralogically Inspired Novel Complex Pb Oxyhalides. *Inorg. Chem.* **2013**, *52*, 12799–12805. [CrossRef]
35. Voropanova, L.A.; Gagieva, Z.A.; Pukhova, V.P.; Vil'ner, N.A. Method of Extracting Lead Ions Pb^{2+} from Acidic Solutions. RU Patent Application No. 2393244C1, 27 June 2010.
36. Lu, H.; Zhang, W.; Yang, Y.; Huang, X.; Wang, S.; Qiu, R. Relative distribution of Pb^{2+} sorption mechanisms by sludge-derived biochar. *Water Res.* **2012**, *46*, 854–862. [CrossRef]
37. Wang, Q.; Zheng, C.; Cui, W.; He, F.; Zhang, J.; Zhang, T.C.; He, C. Adsorption of Pb^{2+} and Cu^{2+} ions on the CS2-modified alkaline lignin. *Chem. Eng. J.* **2020**, *391*, 123581. [CrossRef]
38. Pavlovic, I.; Perez, M.; Barriga, C.; Ulibarri, M. Adsorption of Cu^{2+}, Cd^{2+} and Pb^{2+} ions by layered double hydroxides intercalated with the chelating agents diethylenetriaminepentaacetate and meso-2,3-dimercaptosuccinate. *Appl. Clay Sci.* **2009**, *43*, 125–129. [CrossRef]